Available online at www.sciencedirect.com

SciVerse ScienceDirect

Procedia IUTAM 5 (2012) 144 – 150

Procedia IUTAM

www.elsevier.com/locate/procedia

IUTAM Symposium on 50 Years of Chaos: Applied and Theoretical

Symmetry Induced Heteroclinic Cycles in Coupled Sensor Devices

Antonio Palacios[a*], Visarath In[b], Patrick Longhini[b], Andy Kho[b]

[a]*Nonlinear Dynamical Systems Group, Department of Mathematics, 5500 Campanile Drive, San Diego, CA 92182, USA*
[b]*Space and Naval Warfare Systems Center, Code 2363, 53560 Hull Street, San Diego, CA 92151-5001, USA*

Abstract

In this paper we discuss the existence and stability of heteroclinic cycles in coupled systems and show how they can be exploited to design and fabricate a new generation of highly-sensitive, low-powered, sensor devices. More specifically, we present theoretical and experimental proof of concept that coupling-induced oscillations located near the bifurcation point of a heteroclinic cycle can significantly enhance the sensitivity of an array of magnetic sensors. In particular, we consider arrays made up of fluxgate magnetometers inductively coupled through electronic circuits.

Keywords: Heteroclinic cycles; symmetry; sensors; oscillations

1. Introduction

Loosely speaking, a heteroclinic cycle is a collection of solution trajectories that connects sequences of equilibria, periodic solutions or chaotic invariant sets via saddle-sink connections. For a more precise description of heteroclinic cycles and their stability, see Melbourne et al. [1], Krupa and Melbourne [2], the monograph by Field [3], and the survey article by Krupa [4, 5]. Such behavior is unusual in a general dynamical system. It is, however, a generic feature of dynamical systems that possess symmetry. Indeed, the presence of symmetry can lead to invariant subspaces under which a sequence of saddle-sink connections can be established, resulting in cycling behavior. As time evolves, a typical trajectory would stay for increasingly longer period of time near each solution (which could be either an equilibrium, a periodic orbit or a chaotic invariant set) before it makes a rapid excursion to the next solution. Since saddle-sink connections are robust, these cycles-called heteroclinic cycles-are robust under perturbations that preserve the symmetry of the system.

In this paper we discuss the existence and stability of heteroclinic cycles in coupled systems and show how they can be exploited to design and fabricate a new generation of highly-sensitive, self-powered, sensor devices. More specifically, we present theoretical and experimental proof of concept that coupling-induced oscillations located near the bifurcation point of a heteroclinic cycle can significantly enhance the sensitivity of an array of magnetic sensors. In particular, we consider arrays made up of fluxgate magnetometers inductively coupled through electronic circuits.

*Corresponding author. Tel.: 619-594-6808; fax: 619-594-6746.
Email address: palacios@euler.sdsu.edu (Antonio Palacios)

2210-9838
doi:10.1016/j.piutam.2012.06.018

Report Documentation Page

Form Approved
OMB No. 0704-0188

1. REPORT DATE	2. REPORT TYPE	3. DATES COVERED
2012		**00-00-2012 to 00-00-2012**

4. TITLE AND SUBTITLE	5a. CONTRACT NUMBER
Symmetry Induced Heteroclinic Cycles in Coupled Sensor Devices	5b. GRANT NUMBER
	5c. PROGRAM ELEMENT NUMBER
6. AUTHOR(S)	5d. PROJECT NUMBER
	5e. TASK NUMBER
	5f. WORK UNIT NUMBER
7. PERFORMING ORGANIZATION NAME(S) AND ADDRESS(ES) **Space and Naval Warfare Systems Center,Code 2363, 53560 Hull Street,San Diego,CA,92151**	8. PERFORMING ORGANIZATION REPORT NUMBER
9. SPONSORING/MONITORING AGENCY NAME(S) AND ADDRESS(ES)	10. SPONSOR/MONITOR'S ACRONYM(S)
	11. SPONSOR/MONITOR'S REPORT NUMBER(S)

12. DISTRIBUTION/AVAILABILITY STATEMENT
Approved for public release; distribution unlimited

13. SUPPLEMENTARY NOTES
Procedia IUTAM 5 (2012) 144 - 150

14. ABSTRACT
In this paper we discuss the existence and stability of heteroclinic cycles in coupled systems and show how they can be exploited to design and fabricate a new generation of highly-sensitive, low-powered, sensor devices. More specifically, we present theoretical and experimental proof of concept that coupling-induced oscillations located near the bifurcation point of a heteroclinic cycle can significantly enhance the sensitivity of an array of magnetic sensors. In particular, we consider arrays made up of fluxgate magnetometers inductively coupled through electronic circuits.

15. SUBJECT TERMS

16. SECURITY CLASSIFICATION OF:			17. LIMITATION OF ABSTRACT	18. NUMBER OF PAGES	19a. NAME OF RESPONSIBLE PERSON
a. REPORT	b. ABSTRACT	c. THIS PAGE			
unclassified	**unclassified**	**unclassified**	**Same as Report (SAR)**	**8**	

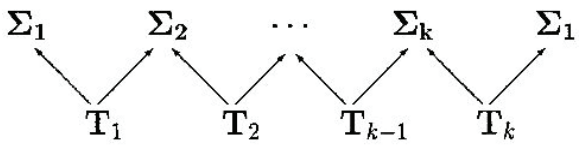

Figure 1: Pattern inside lattice of subgroups that suggests the existence of heteroclinic cycles.

At the center of this discovery is the phenomenon of coupling-induced oscillations, in which the topology of connections, i.e., which sensors are coupled with each other, and the nonlinearities of materials can be exploited to produce self-oscillations that limit in a heteroclinic cycle. This phenomenon is dictated by symmetry conditions alone. In other words, the ideas and methods are device-independent: similar principles can be readily applied to enhance the performance of a wide variety of sensor devices so long as the symmetry conditions are satisfied.

2. Finding Heteroclinic Cycles

For systems whose symmetries are described by the continuous group $\mathbf{O}(2)$, i.e. the group of rotations and reflections on the plane, Armbruster *et al.* [6] show that heteroclinic cycles between steady-states can occur stably, and Melbourne *et al.* [1] provide a method for finding cycles that involve steady-states as well as periodic solutions. Let $\Gamma \subset \mathbf{O}(N)$ be a Lie subgroup (where $\mathbf{O}(N)$ denotes the orthogonal group of order N) and let $g : \mathbf{R}^N \to \mathbf{R}^N$ be Γ-equivariant, that is,

$$g(\gamma X) = \gamma g(X),$$

for all $\gamma \in \Gamma$. Consider the system

$$\frac{dX}{dt} = g(X).$$

Note that $N = kn$ in an n-cell system with k state variables in each cell. Equivariance of g implies that whenever $X(t)$ is a solution, so is $\gamma X(t)$. Using fixed-point subspaces, Melbourne *et al.* [1] suggest a method for constructing heteroclinic cycles connecting equilibria. Suppose that $\Sigma \subset \Gamma$ is a subgroup. Then the fixed-point subspace

$$\mathrm{Fix}(\Sigma) = \{X \in \mathbf{R}^N : \sigma X = X \quad \forall \sigma \in \Sigma\}$$

is a flow invariant subspace. The idea is to find a sequence of maximal subgroups $\Sigma_j \subset \Gamma$ such that $\dim \mathrm{Fix}(\Sigma_j) = 1$ and submaximal subgroups $T_j \subset \Sigma_j \cap \Sigma_{j+1}$ such that $\dim \mathrm{Fix}(T_j) = 2$, as is shown schematically in Figure 1. In addition, the equilibrium in $\mathrm{Fix}(\Sigma_j)$ must be a saddle in $\mathrm{Fix}(T_j)$ whereas the equlibrium in $\mathrm{Fix}(\Sigma_{j+1})$ must be a sink in $\mathrm{Fix}(T_j)$.

Such configurations of subgroups have the possibility of leading to heteroclinic cycles if saddle-sink connections between equilibria in $\mathrm{Fix}(\Sigma_j)$ and $\mathrm{Fix}(\Sigma_{j+1})$ exist in $\mathrm{Fix}(T_j)$. It should be emphasized that more complicated heteroclinic cycles can exist. Generally, all that is needed to be known is that the equilibria in $\mathrm{Fix}(\Sigma_j)$ is a saddle and the equlibria in $\mathrm{Fix}(\Sigma_{j+1})$ is a sink in the fixed-point subspace $\mathrm{Fix}(T_j)$ (see Krupa and Melbourne [2]) though the connections can not, in general, be proved. Since saddle-sink connections are robust in a plane, these heteroclinic cycles are stable to perturbations of g so long as Γ-equivariance is preserved by the perturbation. For a detailed discussion of asymptotic stability and nearly asymptotic stability of heteroclinic cycles, which are also very important topics, see Krupa and Melbourne [2].

Near points of Hopf bifurcation, this method for constructing heteroclinic connections can be generalized to include time periodic solutions as well as equilibria. Melbourne, Chossat, and Golubitsky [1] do this by augmenting the symmetry group of the differential equations with S^1 — the symmetry group of Poincare-Birkhoff normal form at points of Hopf bifurcation—and using phase-amplitude equations in the analysis. In these cases the heteroclinic cycle exists only in the normal form equations since some of the invariant fixed-point subspaces disappear when symmetry is broken. However, when that cycle is asymptotically stable, then the cycling like behavior remains even when the equations are not in normal form. In later work, Buono, Golubitsky, and Palacios [7] proved the existence of heteroclinic cycles involving steady-state and time periodic solutions in differential equations with $\mathbf{D}_n$ symmetry.

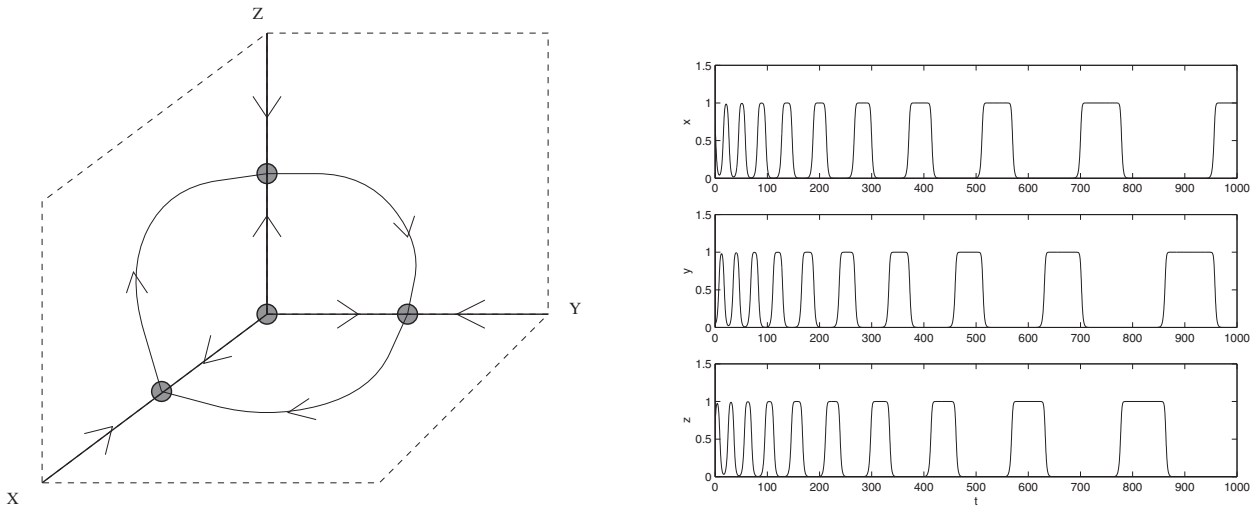

(a) (b)

Figure 2: Heteroclinic cycle found between three equilibrium points of the Guckenheimer and Holmes system. (a) Saddle-sink connections in phase-space, (b) Time series evolution of a typical nearby trajectory. Parameters are: $\mu = 1.0$, $a = 1.0$, $b = 0.55$, $c = 1.5$.

3. The Guckenheimer-Holmes Cycle

Figure 2 illustrates a cycle involving three steady-states of a system of ODE's proposed by Guckenheimer and Holmes [8]. Observe that as time evolves a nearby trajectory stays longer on each equilibrium. The group $\Gamma \simeq \mathbf{Z}_2^3 \otimes \mathbf{Z}_3$ in this example has 24 elements and is generated by the following symmetries

$$(x, y, z) \mapsto (\pm x, \pm y, \pm z)$$
$$(x, y, z) \mapsto (y, z, x)$$

Note that, in fact, this is a homoclinic cycle since the three equilibria are on the group orbit given by the cyclic generator of order 3. The actual system of ODE's can be written in the following form

$$\begin{aligned} \dot{x}_1 &= \mu x_1 - (a x_1^2 + b x_2^2 + c x_3^2) x_1 \\ \dot{x}_2 &= \mu x_2 - (a x_2^2 + b x_3^2 + c x_1^2) x_2 \\ \dot{x}_3 &= \mu x_3 - (a x_3^2 + b x_1^2 + c x_2^2) x_3. \end{aligned}$$

In related work that describes cycling chaos, Dellnitz et al. [9] point out that the Guckenheimer-Holmes system can be interpreted as a coupled cell system (with three cells) in which the internal dynamics of each cell is governed by a pitchfork bifurcation of the form

$$\dot{x}_i = \mu x_i - a x_i^3,$$

where $i = 1, 2, 3$ is the cell number. As μ varies from negative to positive thropugh zero, a bifurcation from the trivial equlibrium $x_i = 0$ to nontrivial equilibria $x_i = \pm\sqrt{\mu}$ occurs.

Guckenheimer and Holmes [8] show that when the strength of the remaining terms in the system of ODE's (which can be interpreted as coupling terms) is large, an asymptotically stable hetroclinic cycle connecting these bifurcated equilibria exists. The connection between the equilibria in cell one to the equilibria in cell two occurs through a saddle-sink connection in the x_1x_2-plane (which is forced by the internal symmetry of the cells to be an invariant plane for the dynamics). As Dellnitz et al. [9] further indicate, the global permutation symmetry of the three-cell system guarantees connections in both the x_2x_3-plane and the x_3x_1-plane, leading to a heteroclinic connection between three equilibrium solutions.

4. A Cycle in A Coupled-Core Fluxgate Magnetometer

4.1. Modeling

In its most basic form, a fluxgate magnetometer consists of two detection coils wound around a ferromagnetic core (usually a single core) in opposite directions to one another [10, 11]. A conventional fluxgate magnetometer, can be treated as a nonlinear dynamical system of the form:

$$\dot{x} = -x + \tanh(c(x + A\sin\omega t + \varepsilon)), \tag{1}$$

where x represents the magnetization state of the core, c is a temperature related parameter, A is the amplitude of the biasing signal with frequency ω and ε is the external magnetic field to be detected. In the absence of a biasing signal, i.e., $A = 0$, and without external signal, i.e., $\varepsilon = 0$, the system dynamics will quickly settle into one of two equilibrium points of (1). For a sufficiently large biasing signal, however, the system may be induced to oscillate. A Coupled-Core Fluxgate Magnetometer (CCFM) is then constructed by *uni*directionally coupling N (odd) wound ferromagnetic cores with cyclic boundary conditions [12], thereby leading to the dynamics,

$$\dot{x}_i = -x_i + \tanh(c(x_i + \lambda x_{i+1} + \varepsilon)), \quad i = 1, \ldots, N \bmod N, \tag{2}$$

where $x_i(t)$ represents the (suitably normalized) magnetic flux at the output (i.e. in the secondary coil) of unit i, and $\varepsilon \ll U_0$ is an external dc "target" magnetic flux, U_0 being the energy barrier height (absent the coupling) for each of the elements (assumed identical for theoretical purposes), the parameter λ represents the strength of coupling between x_i and x_{i+1}.

A bifurcation analysis [13, 12] reveals that the system (2) displays oscillatory behavior with the following features: (A) The oscillations commence when the coupling coefficient exceeds a threshold value

$$\lambda_c = -\varepsilon - x_{inf} + c^{-1}\tanh^{-1} x_{inf}, \tag{3}$$

with $x_{inf} = \sqrt{(c-1)/c}$. Note that in our convention, $\lambda < 0$ (negative feedback) so that oscillations occur for $|\lambda| > |\lambda_c|$. The oscillations are non-sinusoidal, with a frequency that increases as the coupling strength decreases away from λ_c. For $\lambda > \lambda_c$, however, the system quickly settles into one of its steady states, regardless of the initial conditions. The same result ensues if N is even, or if the coupling is bidirectional. For values of λ slightly less than λ_c, there is a small interval $\lambda_{HB} \le \lambda \le \lambda_c$ where global oscillations and synchronous equilibria of the form $(x_1, \ldots, x_N) = (\bar{x}, \ldots, \bar{x})$ can coexist.

The bifurcation diagram for the $N = 3$ case is shown in Fig. 3. It was generated with the aid of the continuation package AUTO [14]. Filled-in circles represent stable oscillations, they emerge via an infinite-period *global* bifurcation that coincides with the creation of a heteroclinic cycle that connects multiple saddle-point equilibria.

At birth the oscillations are fully grown due to the global nature of the bifurcation. As λ approaches λ_c (from the left), so that the strength of the negative feedback is reduced, the oscillation period lengthens and finally becomes infinite at $\lambda = \lambda_c$, when the heteroclinic cycle appears. Empty circles describe unstable oscillations, they all appear via local Hopf bifurcations (labeled HB), so their amplitude increases as a square-root law of the distance from the bifurcation point. Solid (dotted) lines depict stable (unstable) equilibrium points. In particular, the equilibrium points that appear at the pitchfork bifurcation point, labeled B, are all *synchronous*, i.e., of the form $(x_1, x_2, x_3) = (\bar{x}, \bar{x}, \bar{x})$. A close-up view of the interval of bistability of large amplitude oscillations and stable synchronous equilibria is also included. The four branches of unstable equilibria that appear via saddle-node bifurcations (labeled LP) correspond to nonsynchronous equilibria. Collectively, there are fifteen equilibrium points: three synchronous equilibria, including the trivial solution, and twelve nonsynchronous equilibrium points.

(B). The individual oscillations (in each elemental response) are separated in phase by $2\pi/N$, and have period

$$T_i = \frac{N\pi}{\sqrt{cx_{inf}}}\left(\frac{1}{\sqrt{\lambda_c - \lambda}} + \frac{1}{\sqrt{\lambda_c - \lambda + 2\varepsilon}}\right), \tag{4}$$

which shows a characteristic dependence on the inverse square root of the bifurcation "distance" $\lambda_c - \lambda$, as well as the target signal ε. These oscillations can be experimentally produced at frequencies ranging from a few Hz to high kHz.

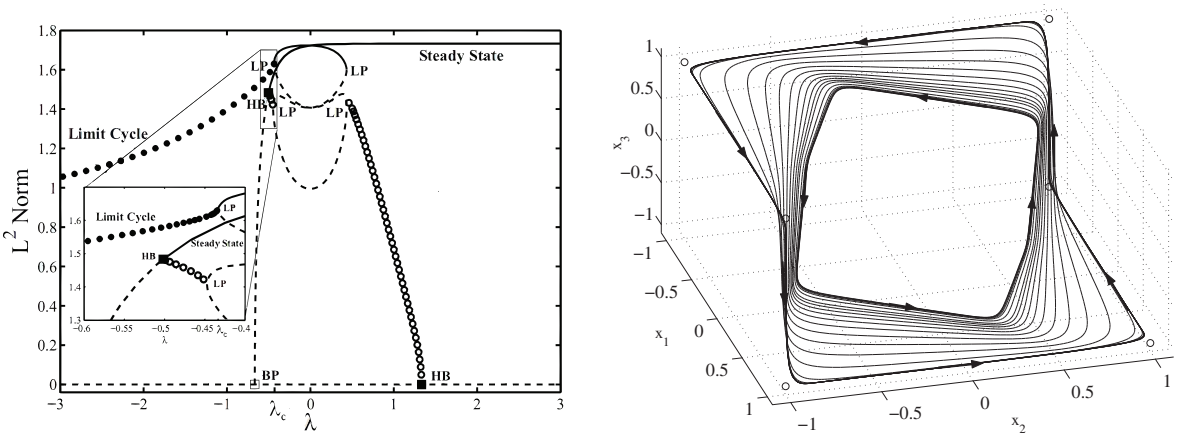

Figure 3: (Left) Bifurcation diagram for a system of three identical bistable elements coupled unidirectionally and without delay. Solid (dotted) lines indicate stable (unstable) equilibrium points. Filled-in (empty) circles represent stable (unstable) periodic oscillations. (Insert) Close-up view of the region of bistability between large-amplitude oscillations and synchronous equilibria. (Right) Family of limit cycles oscillations in phase space. Bold curve corresponds to oscillations very close to the onset of the heteroclinic connection.

(C) The *summed* output oscillates at period $T_+ = T_i/N$ and its amplitude (as well as that of each elemental oscillation) is *always supra* threshold, i.e., the emergent oscillations are strong enough to drive the core between its saturation states, *eliminating* the need to apply an additional bias signal for this purpose, as is done in single-core magnetometers. Increasing N changes the frequency of the individual elemental oscillations, but the frequency of the summed response is seen to be independent of N.
(D) To measure an external signal we rely on a readout mechanism: the Residence Times Detection (RTD), which is based on a threshold crossing strategy of measuring the symmetry-breaking effect of an external signal. Thus under the presence of a target dc signal, the residence times are no longer equal so that either their difference or ratio can be used to quantify the signal. This mechanism is much more sensitive than standard techniques based on the Power Spectra Decomposition because the long-period of oscillations that are characteristic of limit cycles near the onset of a heteroclinic connection renders their wave form highly sensitive to symmetry breaking effects. Then RTD can be computed as $\Delta t \approx \pi\left(1/\sqrt{\lambda_c - \lambda} - 1/\sqrt{\lambda_c - \lambda + 2\varepsilon}\right)/\sqrt{cx_{inf}}$, which vanishes (as expected) for $\varepsilon = 0$, and can be used as a quantifier of the target signal, analogous to the time-domain operation of the single fluxgate.
(E) The system responsivity, defined via the derivative $\partial\Delta t/\partial\varepsilon$, is found to increase dramatically as one approaches the critical point in the oscillatory regime; this suggests that careful tuning of the coupling parameter so that the oscillations have very low frequency, could offer significant benefits for the detection of very small target signals. For small target signals, one may do a small-ε expansion to yield $\Delta t \approx \pi\varepsilon(\lambda_{c0} - \lambda)^{-3/2}/\sqrt{cx_{inf}}$, where λ_{c0} now represents the critical coupling, absent the target signal. For a fixed ε, one observes, immediately, that the responsivity $\partial\Delta t/\partial\varepsilon$ increases as one approaches the critical point (through adjusting the coupling parameter λ). The instrument thus yields its optimal performance in the very low frequency regime, close to the oscillation threshold; it is worth noting that the experimental system can be made to oscillate at very low frequencies (around 65hz), far lower than the bias frequency for conventional fluxgates. The coupled system can be "tuned" to this regime by adjusting the coupling coefficient λ.

4.2. Design and Fabrication

Figure 4 shows an actual realization of a CCFM with three fluxgate magnetometers coupled uni-directionally. The PCB (printed circuit board) technology based cores are made of Cobalt-based Metglas 2714A material, and each is sandwiched between two sheets of PCB material. The sides of the PCB sheets that face away from the core material are printed with copper wirings to form the windings for the driving and sensing coils. Solder is used to fuse the two sheets together to complete the circuit for the windings. The cores are then coupled through electronic circuits where the (voltage) readout of one fluxgate signal (i.e., the derivative signal of the flux detected by the sensing coil) is amplified by a voltage amplifier with a very high impedance, which also trims out any dc signal in the output.

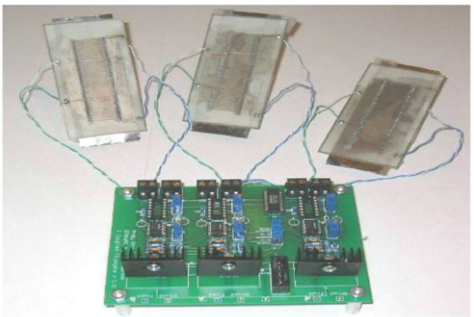

Figure 4: Prototype design of a coupled core fluxgate magnetometer with three fluxgates.

Following this, the signal is passed through a leaky integrator to convert the derivative signal seen by the sensing coil back to the "flux" form so that the experimental system closely conforms to the model (2).

Typically, the integrator output contains a dc component that must be removed before the signal is passed to the other fluxgates. This is accomplished by employing a Sallen-Key second-order high pass filter immediately after the integrator. The signal then passes through an amplifier to achieve adequate gain to drive the adjacent fluxgate. After this, the signal passes through a voltage-to-current converter (V-I converter) in its final step to drive the primary coil of the adjacent fluxgate. The setup repeats for the remaining two fluxgates and all values of the coupling circuit parameters are closely matched from one set to the other.

The oscillations observed from this setup are quite striking, see Fig. 5. The system readily oscillates in a travelling pattern. Like the model, the system favors this pattern no matter how many times it is restarted. The frequency of oscillations is about 33.5 Hz. Each wave is phase shifted by exactly $\frac{2\pi}{3}$ as predicted by the model. Comparison of the oscillations from the experiment to the numerical results shows good agreement. In addition, since we do not know the value of c and the time constant τ in the actual device (we set $\tau = 1$ in the model), we cannot correctly compare the time scales in the model and the experimental observations. The amplitudes of the oscillations in the experiment are also arbitrary compared to the model because the recorded voltages depend on the gains set in the coupling circuit. On the other hand, the magnetic flux in the model saturates between ± 1, but in the fluxgate devices, this quantity cannot be measured directly.

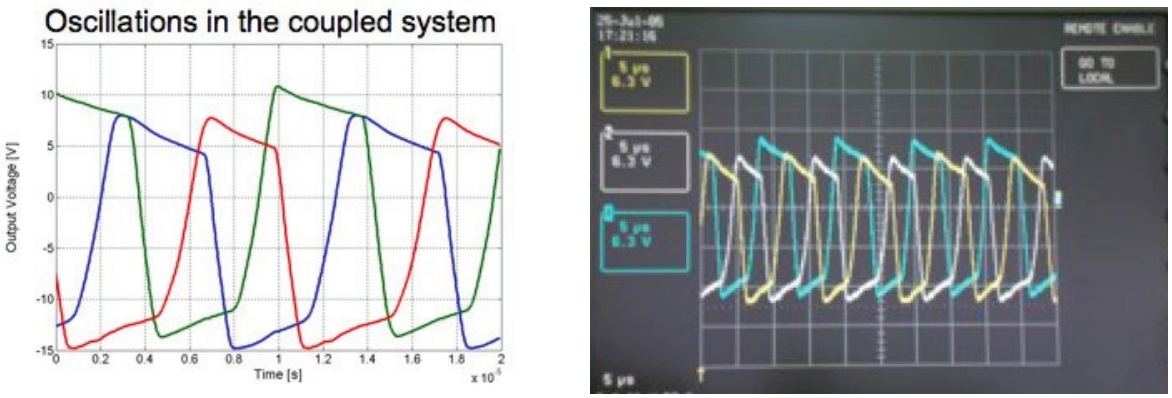

Figure 5: Comparison of voltage oscillations obtained near the onset of a heteroclinic connection in (left) computer simulations of a CCFM modeled by Eq. (2) show good agreement with (right) experimental voltage measurements of prototype of a CCFM device tuned up to operate near the heteroclinic cycle.

5. Conclusions

Heteroclinic connections in phase space are rather rare features of dynamical systems because they require solution trajectories to make complex excursions among many different solutions sets, i.e., steady-states, periodic solutions, and even chaotic sets. They are, however, ubiquitous in dynamical systems that posses symmetry. Indeed, symmetry facilitates the creation of invariant regions through which solution trajectories can make repeated excursions in a more natural way. Over the past ten years we have conducted various analytical, computational, and experimental works to investigate the fundamental idea that coupling-induced oscillations that emerge through heteroclinic connections can be exploited to develop a new generation of highly-sensitive, low powered, dynamic sensors. In this work we use the fluxgate magnetometer, which is essentially a coil sensor with a ferromagnetic core, as case study to illustrate the basic ideas and methods to enhance sensor performance. The individual fluxgates are coupled uni-directionally via magnetic flux. This type of coupling configuration favors, for certain coupling strengths, the existence of structurally stable heteroclinic cycles that involve saddle-sink connections between multiple equilibrium points. More importantly, the cycles are accompanied by a branch of globally stable limit cycle oscillations. At birth, these oscillations are fully grown with a large amplitude, which distinguishes them from the slowly growing oscillations that emerge via Hopf bifurcations. This is a critical feature to enhance performance because the large period, large amplitude, oscillations that typically occur near the onset of a heteroclinic connection render the collective oscillations highly sensitive to symmetry-breaking effects caused by external signals. An experimental prototype of a CCFM device yields voltage oscillations that are in very good agreement with computer simulations of the model equations. More importantly, the sensitivity of device is significantly stronger than that of a single unit, as expected.

Acknowledgements

The authors acknowledge support from the SPAWAR internal funding (ILIR) program and the Office of Naval Research (Code 331). The work of AP was supported in part by National Science Foundation grants CMMI-0638814 and CMMI-0625427.

References

[1] I. Melbourne, P. Chossat, M. Golubitsky, Heteroclinic cycles involving periodic solutions in mode interactions with **o(2)** symmetry, Proc. Roy. Soc. of Edinburgh 113A (1989) 315–345.
[2] M. Krupa, I. Melbourne, Asymptotic stability of heteroclinic cycles in systems with symmetry, Ergod. Th. & Dynam. Sys. 15 (1995) 121–147.
[3] M. Field, Lectures on Bifurcations, Dynamics and Symmetry., Vol. 356 of Pitman Res. Notes, Addison-Wesley Longman Ltd., Harlow, 1996.
[4] M. Krupa, Robust heteroclinic cycles, J. Nonlin. Sci. 7 (2) (1997) 129–176.
[5] M. Krupa, Bifurcations of relative equilibrias, SIAM J. Math. Anal. 21 (1990) 1453–1486.
[6] D. Armbruster, J. Guckenheimer, P. Holmes, Heteroclinic cycles and modulated traveling waves in systems with o(2) symmetry, Physica D 29 (1988) 257–282.
[7] P. L. Buono, M. Golubitsky, A. Palacios, Heteroclinic cycles in rings of coupled cells, Physica D 143 (2000) 74–108.
[8] J. Guckenheimer, P. Holmes, Structurally stable heteroclinic cycles, Math. Proc. Camb. Phil. Soc 103 (1988) 189–192.
[9] M. Dellnitz, M. Field, M. Golubitsky, J. Ma, A. Hohmann, Cycling chaos, Int. J. Bifurc. Chaos 5 (4) (1995) 1243–1247.
[10] P. Ripka, Review of fluxgate sensors, Sensors and Actuators A 33 (1996) 129–141.
[11] P. Ripka, Advances in fluxgate sensors, Sensors and Actuators A 106 (2003) 8–14.
[12] V. In, A. Bulsara, A. Palacios, P. Longhini, A. Kho, J. Neff, Coupling induced oscillations in overdamped bistable systems, Physical Review E 68 (2003) 045102–1–0415102–4.
[13] A. Bulsara, V. In, A. Kho, P. Longhini, A. Palacios, W. Rappel, J. Acebron, S. Baglio, B. Ando, Emergent oscillations in unidirectionally coupled overdamped bistable systems, Physical Review E 70 (2004) 036103.
[14] E. Doedel, X. Wang., Auto94: *Software for Continuation and Bifurcation Problems in Ordinary Differential Equations*, Applied Mathematics Report, California Institute of Technology.